ELSEVIER

Mercury bioremediation in aquatic environment by genetically modified bacteria with self-controlled biosecurity circuit

Yubin Xue [a], Pei Du [b], Amal Amin Ibrahim Shendi [c], Bo Yu [a,d,*]

[a] *CAS Key Laboratory of Microbial Physiological and Metabolic Engineering, State Key Laboratory of Mycology, Institute of Microbiology, Chinese Academy of Sciences, Beijing, 100101, China*
[b] *CAS Key Laboratory of Pathogen Microbiology and Immunology, Institute of Microbiology, Chinese Academy of Sciences, Beijing, 100101, China*
[c] *Polymers and Pigments Department, Chemical Industries Division, National Research Centre, Dokki, Cairo, Egypt*
[d] *CAS-TWAS Centre of Excellence for Biotechnology, Beijing, 100101, China*

ARTICLE INFO

ABSTRACT

Heavy metal pollution such as mercury (Hg^{2+}) poses a severe threat to food security worldwide because of enrichment through food chain and, eventually, to the human body. Biological remediation approaches are promising, but in some cases, the natural microorganisms are not ideal for practical application, which requires genetic modification of such organisms. However, the threat of genetically modified bacteria being released into the environments has long been the major concern that limits the applications of such technologies. In this study, we designed and optimized a genetic circuit that is capable of activating a Hg^{2+} adsorption module after sensing Hg^{2+} in waterbody, and killing cells with a cell suicide module in a programmable manner. With this circuit, the engineered *Escherichia coli* cells are programmed to express Hg^{2+} adsorption protein only when Hg^{2+} concentration is above a certain threshold. Then, cells absorbed with Hg^{2+} can be removed from natural environments with magnetically immobilized strategy and the remaining cells are programmed to be killed by the suicide module when Hg^{2+} concentration drops below a threshold in waterbody. Importantly, the suicide module was carefully optimized to ensure the escape rate is below 10^{-9}, which meets the recommendation demanded by U.S. NIH guideline. The absorption cells could be reused for 5 cycles, with an Hg^{2+} adsorption efficiency steadily above 95% and escape rates below 10^{-9}. Thus, the advancement of this study sheds light on using engineered microbes directly in an open circumstance.

1. Introduction

Environmental pollution from hazardous waste materials, organic pollutants and heavy metals, has adversely affected the natural ecosystem to the detriment of human beings. Urgent environmental problems compelled people to seek for novel strategies to protect and remediate the polluted environments, such as plastic degradation (Cui et al., 2021), heavy metal remediation (Zhu et al., 2020) as well as ecosystem conservation (Redford et al., 2019). The nondegradable character distinguished heavy metals from other contaminants and made them difficult to eliminate from the environment. The rapid industrialization in recent years has resulted in severe heavy metal pollution, which is disastrous to the environment. Removal of these heavy metal pollution has become an urgent task. Conventional physical and chemical methods are expensive and not effective in areas with low metal toxicity or unable to permanently remove the pollution from environment. Bioremediation is therefore an eco-friendly and efficient method of reclaiming environments contaminated with heavy metals. Microbiological treatments have gained increasing attentions because of their cost-effectiveness and environmentally friendliness. Although lots of microbes isolated from natural sources have been applied for environmental remediation, the efficiency of natural organisms normally could not meet actual industrial requirements, especially in the case of emergencies when pollutants are highly concentrated and need to be cleaned up in a short time. Notably, besides heavy metals, there are still some pollutants released to the environment, which natural organisms could not remediate them. Thus, researchers have been improving the technologies of bioremediation to meet the demands, for example, using

---

genetically modified microorganisms (GMOs) (Brune and Bayer, 2012). It is indisputable that genetically engineered bacteria are more efficient in the bioremediation processes (Pant et al., 2021). However, once GMOs are released into environment, these artificial livings might have unpredictable impacts to the environment. GMOs may disturb the stability of microbial community (Dana et al., 2012); influent the diversity of wild germplasm resources (Quist and Chapela, 2001) as well as causing public panic (Redford et al., 2013). Thus, use of GMOs for environmental bioremediation is strictly regulated by current policies and laws. The U.S. National Institutes of Health (NIH) guideline recommended that an acceptable GMOs escape rate should be kept below 10^{-8} (Wilson, 1993).

Considering the bio-threats from GMOs released into environments, to date, these technologies are still limited in the laboratory research stage. While traditional studies on transgenic microbes took biosafety into account (Sayler and Ripp, 2000), researchers rarely demonstrated the theories of genetic safeguard systems (Moe-Behrens et al., 2013), which were with low stability and could not meet NIH substandard. Nowadays, synthetic biology is accelerating the iterative update of industry, agriculture development and drug research, as well as the environment microbiological technologies (Khalil and Collins, 2010). With the continuous advancement of synthetic biology, it is now possible to control the behavior of cells, including procedural expression of the functional genes and cell death (Hossain et al., 2020). Thus, this opens up windows to expand the applications of GMOs with controllable behaviors.

In this study, a biocontainment circuit tightly controlled by a logical NOR gate is designed and optimized for conditionally triggering suicide of the *Escherichia coli* strain after completing the work or once escaping into the natural environments by an accident. As the research on Hg^{2+} remediation is more common than other toxic heavy metal ions, we simply choose Hg^{2+} bioremediation as an example to demonstrate this design. The designed circuit could automatically sense the variation of Hg^{2+} concentrations in the waterbody and start to express Hg^{2+} adsorption proteins. Once the genetically modified bacteria finished the cleaning work, or escaped to the natural environment, the expression of the suicide module will be automatically activated when the concentration of Hg^{2+} in the environment is too low to inhibit the suicide gene expression, thereby realizing the programmed suicide of the cells. After careful optimization of the sensitivity of the circuit, we achieved an escape rate as low as 10^{-9} in this study, which meets the recommendation demand of U.S. NIH guideline. This work would provide toolboxes for rational design of biosecurity system in gram-negative strains and also shed light on the bioremediation fields by directly using engineered microbes in an open environment.

2. Material and methods

2.1. Strains and cultivation conditions

E. coli TOP10 was used as the host strain for plasmid construction and genetic circuit characterization. Strains and plasmids used in this study are listed in Table 1. Strains were cultivated in Luria-Bertani (LB) medium. Antibiotics including apramycin, ampicillin, kanamycin and chloramphenicol supplemented with appropriate concentration (100, 50, 25, 12.5 μg/mL, respectively), as required. To maintain the survival state of strains containing circuit for cell suicide, 1 mM of isopropyl-beta-D-thiogalactopyranoside (IPTG) or 1 μM Hg^{2+} ions were added into the medium. For triggering immediately cell death, a final concentration of 100 nM anhydrotetracycline (ATc) were added when IPTG or Hg^{2+} were absent in the medium.

2.2. Genetic manipulations

Two basic plasmids for regulating functional genes expression (pRG) and programable toxin genes expression (pPT) were inherited from a

Table 1
Strains and plasmids used in this study.

Strains or plasmids	characteristics/purposes	Source
Strains		
Escherichia coli TOP10	K-12 F- mcrA Δ(mrr-hsdRMS-mcrBC) φ80lacZΔM15ΔlacX74 nupG recA1 araD139 Δ(ara-leu)7697 galE15 galK16 rpsL(StrR) endA1 λ-	Biomed Co. Ltd.
E. coli TOP10SS	*E. coli* TOP10 186 attB::P$_{Tac}$-TetR	This work
E. coli SS1.0	*E. coli* TOP10SS harboring plasmids of p2015a-P$_{MerT}$-TetR-INP-CL and pPT-P$_{LtetO}$-50-ecoRI	This work
E. coli SS2.0	*E. coli* TOP10SS harboring plasmids of p2015a-P$_{MerT}$-TetR-INP-CL-Term-P$_{LtetO}$-50-ecoRI and pSEVA221-P$_{LtetO}$-50-doc	This work
E. coli SS3.0	*E. coli* TOP10SS harboring plasmids of p2015a-P$_{MerT}$-TetR-INP-CL-Term-P$_{LtetO}$-50-ecoRI, pSEVA221-P$_{LtetO}$-50-doc and pBAC-PLtetO-50-doc	This work
Plasmids		
pRG	IPTG inducible P$_{Tac}$ promoter expression vector p15A ori, Amp^R	Zong et al., (2017)
pPT	pSB4C5 derived output plasmid with insulated promoter cores, pSC101 ori, Cm^R	Zong et al., (2017)
pOSIP-KO	one step chromosomal integration plasmid targeting *E. coli* phage 186 attB, Kan^R	St-Pierre et al. (2013)
pE-FLP	Flp based antibiotic-resistance scar excision plasmid, Amp^R	St-Pierre et al. (2013)
p2015a	pRG derived broad-host-range medium copy plasmid, pRO1600 ori, Amp^R	This work
p2015a-P$_{Tac}$-sfGFP	p2015a carrying LacI-P$_{Tac}$-sfGFP	This work
p2015a-P$_{Tac}$-TetR	p2015a carrying LacI-P$_{Tac}$-TetR	This work
p2015a-LacZ-sfGFP	p2015a carrying LacZ-sfGFP	This work
p2015a-10333	p2015a carrying J103-33MerR-P$_{MerT}$-sfGFP	This work
p2015a-10933	p2015a carrying J109-33MerR-P$_{MerT}$-sfGFP	This work
p2015a-11533	p2015a carrying J115-33MerR-P$_{MerT}$-sfGFP	This work
p2015a-10533	p2015a carrying J105-33MerR-P$_{MerT}$-sfGFP	This work
p2015a-10833	p2015a carrying J108-33MerR-P$_{MerT}$-sfGFP	This work
p2015a-10033	p2015a carrying J100-33MerR-P$_{MerT}$-sfGFP	This work
p2015a-108R0	p2015a carrying J108-RBS$_{opt}$-MerR-P$_{MerT}$-sfGFP	This work
p2015a-10832	p2015a carrying J108-32MerR-P$_{MerT}$-sfGFP	This work
p2015a-10834	p2015a carrying J108-34MerR-P$_{MerT}$-sfGFP	This work
p2015a-10830	p2015a carrying J108-30MerR-P$_{MerT}$-sfGFP	This work
p2015a-P$_{MerT}$-TetR-INP-CL$_5$	p2015a-108R0 carrying optimized absorption & signal processing parts	This work
p2015a-P$_{MerT}$-TetR-INP-CL-Term-P$_{LtetO}$-50-ecoRI	p2015a-108R0 carrying optimized absorption & signal processing parts, and an *Eco*RI based biocontainment part	This work
pPT-P$_{LtetO}$-sfGFP	pPT carrying P$_{LtetO}$-sfGFP	This work
pPT-P$_{LtetO}$-50-ccdB	pPT carrying P$_{LtetO}$-50-ccdB	This work
pPT-P$_{LtetO}$-50-ecoRI	pPT carrying P$_{LtetO}$-50-ecoRI	This work
pPT-P$_{LtetO}$-50-doc	pPT carrying P$_{LtetO}$-50-doc	This work
pSEVA221-P$_{LtetO}$-50-doc	pSEVA221 carrying P$_{LtetO}$-50-doc, KanR	This work
pBAC-P$_{LtetO}$-50-doc	pBAC carrying P$_{LtetO}$-50-doc, AprR	This work
pOSIP-KO-P$_{Tac}$-TetR	pOSIP-KO carrying LacI-P$_{Tac}$-TetR, KanR	This work

previous research (Zong et al., 2017). To implement gene regulation under multiple environments, the genetic circuit activated by Hg^{2+} or IPTG was created on pRG derivate vector p2015a. The IPTG inducible plasmid named p2015a-*P$_{Tac}$-sfGFP* and p2015a-*P$_{Tac}$-TetR* were constructed to choose an appropriate IPTG level for activating the LacI regulated promoter *P$_{Tac}$*. Furthermore, for cultivation of plasmids containing toxin genes, the *P$_{Tac}$-TetR* cassette was integrated into chromosome of *E. coli* TOP10, resulting strain TOP10SS (TOP10 Survival State)

through one step genome integration method (St-Pierre et al., 2013). When cultivated in presence of IPTG, the expression of suicide modules was transcriptionally inhibited under the tightly regulation of TetR. Plasmids p2015a-P_{Tac}-INP-MerR, p2015a-P_{Tac}-INP-CL$_5$ were constructed for testing the functionalities of the selected bioremediation elements. For verifying the optimum Hg^{2+} inducible element, a series of MerR-P_{MerT} promoters were introduced into p2015a for construction of whole-cell mercury biosensors. The Hg^{2+} activating plasmids, p2015a-P_{MerT}-TetR and p2015a-P_{MerT}-PhlF, were designed for demonstration of the basal amount mercury ions for completely turning OFF the suicide action, along with plasmids pTP-P_{LtetO}-sfGFP and pTP-P_{PhlFO3}-sfGFP. Basing on the characterization results of Hg^{2+} and IPTG inducible promoters, plasmid harboring entire elements except the suicide gene, p2015a-P_{MerT}-TetR-INP-CL$_5$, were constructed as the final version of functional Hg^{2+} remediation vector.

To realize the programable expression of suicide gene, two plasmids consisting of repressible promoters P_{LtetO} and a further hybrid promoter $P_{LtetO-PhlFO3}$ were firstly performed on the plasmid backbone pPT for screening an optimized NOR logical gate. The well characterized $P_{LtetO-1}$ promoter was used for constructing NOR gate (Lutz and Bujard, 1997), and then the toxin genes ecoRI (Torres et al., 2003), ccdB (Smith and Maxwell, 2006), doc (Liu et al., 2008) with different strengths of RBSs (ribosome binding sites) were cloned into TOP10SS strain. Similarly, for achieving the biocontainment efficiency according to the NIH guideline, the P_{LtetO}-doc cassette with best killing efficiency were cloned to pBAC and pSEVA221 vectors. All plasmids mentioned above were created using Gibson Assembly or Golden Gate Assembly methods (Engler et al., 2008; Gibson et al., 2009).

The first version of biosorption strain, *E. coli* SS1.0 was constructed by introducing plasmids p2015a-P_{MerT}-TetR-INP-CL and pPT-P_{LtetO}-50-ecoRI into TOP10SS strain, which contained precisely tuned expression of negative regulatory protein TetR as well as the Hg^{2+} capture element INP-CL. The second version strain *E. coli* SS2.0 was improved by combining the plasmid p2015a-P_{MerT}-TetR-INP-CL-Term-P_{LtetO}-50-ecoRI and an additional low copy plasmid pSEVA221-P_{LtetO}-50-doc. The final version of strain *E. coli* SS3.0 was constructed with additional redundant 2 copies of doc and one copy of ecoRI gene to achieve high biocontainment efficiency. To fulfill this, three plasmids of p2015a-P_{MerT}-TetR-INP-CL-Term-P_{LtetO}-50-ecoRI, pSEVA221-P_{LtetO}-50-doc and pBAC-PLtetO-50-doc were transformed into *E. coli* TOP10SS strain. The detailed information of the above-mentioned plasmids could be referred to Table 1.

2.3. Growth conditions and fluorescence analysis

Overnight cultures (2×10^9 CFU/mL) were inoculated in LB broth at an initial cell density of 2×10^7 CFU/mL (dilution rate of 1:100) and grown at 37 °C, 200 rpm for 16–18 h. For mercury or IPTG inducible dose-response curve measurements, cells were firstly inoculated for 3 h in LB until cell density reached to 6×10^8 to 8×10^8 CFU/mL. Then different amounts of inducers were added and grown for another 3 h. The used gradient concentrations of inducer were 0, 0.01, 0.02, 0.05, 0.1, 0.2, 0.5, 1, 2, 5, 10 μM for Hg^{2+} and 1, 2, 5, 10, 20, 50 μM for IPTG. Cultures were collected by centrifugation at 6,000 rpm for 10 min. Pellets were washed twice using phosphate buffer solution (PBS, pH = 7.0), and the fluorescence data were recorded by the microplate reader (Thermo Scientific, 485 nm for excitation and 520 nm for emission).

2.4. Mercury absorption assays

In order to identity the optimized mercury absorption elements for genetic circuits, the peptides with Hg^{2+} binding ability were surface-displayed expression on the cell surface of *E. coli* strain by using the *N*-terminal region of ice-nucleation gene *inaK* from *Pseudomonas syringae* (INP) as the anchor protein (Li et al., 2004). The recombinant strains were cultivated to a final cell density of 2×10^9 CFU/mL in LB medium

with 0.5 mM IPTG to promote the protein expression. Then, the cells were harvested and washed twice using PBS (pH = 7.0) and resuspended in 100 mM PBS at a final concentration of 1×10^9 CFU/mL. The artificial Hg^{2+} polluted wastewater was used, which was prepared freshly for each time by adding Hg^{2+} into 0.9% saline solution. To determine the mercury absorption capacities by free cells, 50 μM Hg(NO$_3$)$_2$ were added and incubated for 1 h. After centrifuged at 6,000 rpm for 10 min, the residual Hg^{2+} were immediately measured by Water Mercury Ion (Hg^{2+}) Content Assay Kit (Beijing Solarbio Science & Technology, China) with a spectrophotometer at the wavelength of 490 nm.

For preparation of immobilized cells, the cells were first cultivated as mentioned above. Twenty gram per liter of strontium ferrite (SrFe$_{12}$O$_{19}$) distributed in 4 g/L sodium alginate mixed with cell suspension to the final cell density of 3×10^{10} CFU/mL was extruded into 2% CaCl$_2$ and solidified for 2 h. Then the prepared magnetic immobilized particles were applied for Hg^{2+} adsorption and used repeatedly. Each cycle of mercury absorption experiment was performed in 10 mL solution (10 μM Hg^{2+} in 0.9% saline solution) addition with 10% volume of immobilized particles for 12 h at 28 °C. The cell activity was defined as the ratio of decreased amount of mercury concentration in the supernatant to the initial Hg^{2+} concentration in the solution. Then, cells were harvested by magnetic separation and re-activated in 0.9% saline with 0.1% glucose for 12 h, prior to next cycle of treatment.

2.5. Cell escape rate assays

E. coli strains harboring toxin plasmids or negative control plasmids were cultivated overnight in LB with appropriate antibiotics. Five microliter of each dilution (from 10^0 to 10^{-7}) was spotted onto LB plates with or without 0.5 μM Hg^{2+} ions, and the cells survival ratio equals to the proportion of survived CFU under nonpermissive condition to the total CFU under permissive condition. Each experiment was performed with three replicates. Cells containing the final version of biocontainment circuit transformants were activated under survival conditions. One mL cultures of OD$_{600}$ = 1.0, which equals to about 10^9 cells, were washed, resuspended twice and then put onto LB plates supplied with appropriate antibiotics for calculating CFU and survival ratios. The escape rate was defined as the average number of colonies survival on LB antibiotic plates per 10^9 cells.

2.6. Scanning electron microscope analysis

Surface properties of cells loaded with SrFe$_{12}$O$_{19}$ nano-magnetic particles of the calcium alginate beads was characterized by using scanning electron microscope (SEM) analysis. Samples was washed twice with ddH$_2$O, and fixed with 2.5% glutaraldehyde at 4 °C overnight. Fixed samples were dehydrated through different concentration of ethanol solution with a gradient (30%, 50%, 70%, 80%, 90%, 95%, 100%) for 15 min each and finally washed by pure ethanol twice. Samples were further treated through critical point drying and coated with gold before scanning electron microscope analysis. Electron micrographs were obtained from the Hitachi SU8010 SEM (Tokyo, Japan).

3. Results and discussion

3.1. Designing an intelligent circuit for programed mercury adsorption and cell death

Heterologous expression of protein might trigger metabolic burden in the cells, which leads to undesirable physiological changes. Thus, dynamic regulatory systems are useful for alleviating such burden, especially when many foreign genes are introduced into cells (Wu et al., 2016). A possible solution to such problem is using genetic circuit to control gene expression in a programmable manner. MerR, as an inhibitor protein, is the Hg-sensing transcription factor that regulates expression by coupling the promoter of P_{merT}. This regulator was shown

to be an activator of P_{merT} in the presence of Hg^{2+} and a weak repressor in the absence of Hg^{2+} (Brown et al., 2003). Upon Hg^{2+} binding, MerR undergoes extensive conformational changes that lead to the assembly of Hg^{2+} binding site, and dissociates from P_{merT} and then activates the promoter. Özyurt et al. (2019) recently developed a fluorescent biosensor by fusing MerR and enhanced yellow fluorescent protein to detect Hg^{2+} in drinking water.

We then designed a genetic circuit based on the knowledge of *MerR-P_{merT}* system. The circuit could sense the Hg^{2+} concentration variations in the environment and automatically triggers specific gene expression to realize a programmable control of the expression of Hg^{2+} absorption and cell death module (Fig. 1). As shown in the box of Sensor 1, the constitutive promoter P_c is used to initiate the normal expression of MerR protein, and thus shut down the expression of genes downstream of P_{merT} to avoid metabolic burden in the absence of Hg^{2+} ions. Once the concentration of environmental Hg^{2+} ions rise above a certain threshold, MerR will dissociate which allows activation of P_{merT} to express Hg^{2+} binding protein (MBP) and start the absorption of Hg^{2+} ions (Effector 1, the bioremediation part). Meanwhile, TetR, a negative regulatory protein of the P_{LtetO} promoter, will also be expressed by P_{merT} promoter (Terpe, 2006). Thus, in the presence of Hg^{2+} ions, the toxin gene driven by P_{LtetO} promoter cannot be expressed, which allows the bacteria to proliferate normally. In the later stage of water treatment, when cells have been recovered from the aquatic environment and the concentration of Hg^{2+} ions in the waterbody have dropped below the threshold of the promoter response, the P_{merT} promoter will be repressed again and stop the expression of MBP and TetR. Subsequently, as cells continue to reproduce, the intracellular TetR protein concentration will be diluted and, eventually, disappear. As a result, the P_{LtetO} promoter will be activated again to express the toxin genes (Effector 2, the bio-containment part), which ensures the death of GMOs and thereby achieves environmental bio-safety.

Additionally, considering the fact that Hg^{2+} could inhibit cell growth, the circuit also has another part only used for seed culture. As shown in the box of Sensor 2 in Fig. 1, IPTG is only required in the seed culture step. The P_{LtetO} promoter is tightly regulated by the LacI and TetR double negative regulatory protein system to completely shut down the expression of the toxin gene. This module ensures normal cultivation of cells without Hg^{2+} addition. Once the strains were applied into the Hg^{2+} contaminated environments, Hg^{2+} would take charge through P_{merT} promoter for continuous production of TetR to inhibit toxin gene expression. Thus, the circuit has achieved the function of a NOR logic gate. With the presence of either IPTG or Hg^{2+}, expression of the toxin will be repressed, and cells can survive to proliferate in seed culture or

absorb Hg^{2+} in contaminated water respectively. On the other hand, cells are programmed to die by expressing toxins.

3.2. Optimization of multiple-input logic gate and tightly controlled anti-escape system

After *in silico* design, realizing the circuit first relies on qualified parts with high sensitivity. Thus, we first optimized the sensitivity of each module. *E. coli* strains have been reported to tolerant a Hg^{2+} concentration up to 10 μM (Tay et al., 2017), while the typical concentration of mercury ions in contaminated water are relatively lower, varying from 10 to 100 nM level (Zhang et al., 2018). MerR based mercury biosensors have been widely used on mercury sensing for their high selectivity. Other biosensors, like P_{cadR} (Tao et al., 2013) or P_{golTS} (Cerminati et al., 2015), also showed promising detection limits of respective 1.6 μM and 4.4 nM, but have lower selectivity since they could also be activated by other irons like Zn^{2+}, Cd^{2+}, and Pb^{2+}. The genetic architecture of Hg^{2+} biosensor contains a continuously expressed MerR protein and promoter P_{merT}. However, the Hg^{2+} detection limit of putative P_{MerT} promoter is over 1 μM (Wang et al., 2013), and few research has been done for optimizing the sensitivity of P_{MerT}. Such response concentration is too high to match the typical mercury concentration in waterbody, which requires fine-turning of the gene expression level of *merR* to adjusting the response sensitivity of P_{merT} promoter.

We first tuned intracellular MerR concentration by selecting a series of constitutive promoters and RBS with various strengths (Wan et al., 2019). Several promoters from Anderson's promoter library (http://parts.igem.org/) and 5 RBSs designed by RBS Calculator (https://salislab.net/software) with various strengths were placed in front of *merR* gene and green fluorescence protein (*sf*GFP) was used as a reporter gene for P_{merT}. Up to 10 promoter/RBS combinations were evaluated under a set of mercury concentrations from 10 nM to 10 μM to screen for the ones with higher output, dynamic range as well as lower leakage based on the dose response curves. As shown in Fig. 2a, before optimization, the expression strength of most suboptimal promoter/RBS pairs for MerR are too high (such as J_{108}-rbs$_{30}$) or too low (such as J_{114}-rbs$_{33}$). The incompatible amount between intercellular MerR and promoter P_{MerT} lead to poor sensitivity (K_M about 2–5 μM) as well as mild changes response to Hg^{2+} changing (Hill coefficient n only 1.5). The performances of all the promoter/RBS combination for MerR expression were characterized in Table 2. To sum up, the optimal combination consists of a strong promoter and a weak RBS. The highest intracellular MerR concentration of the mercury sensing module was achieved while using the middle strength promoter J_{108} and an artificial RBS (rbs$_{op}$) with a
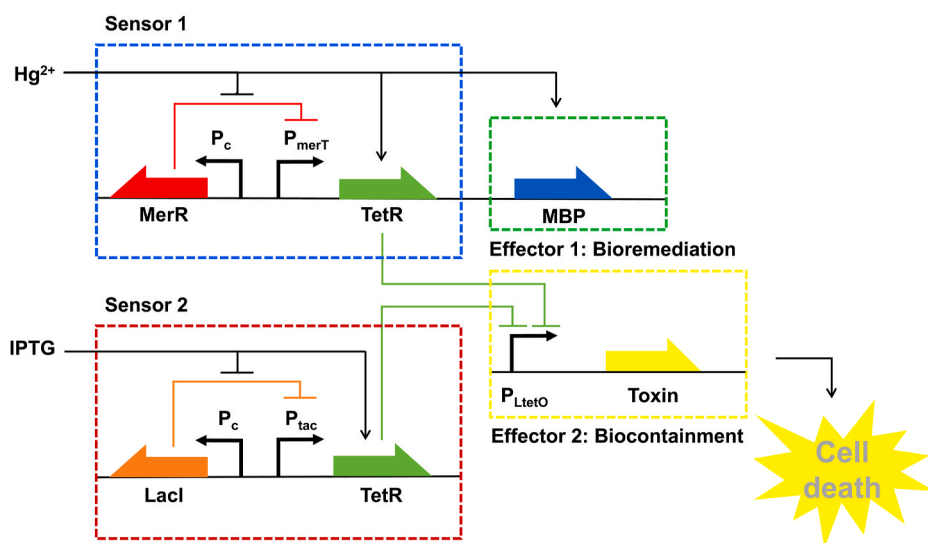

Fig. 1. Schematic of genetic circuit for bioremediation and biocontainment system.

Sensor 1, Hg^{2+} responsive module and Sensor 2, IPTG responsive module; Effector 1, mercury binding protein (MBP) for bioremediation and Effector 2, suicide protein (toxin) for biocontainment function. P_c, constitutive promoter; P_{MerT}, mercury inducible promoter; P_{Tac}, IPTG inducible synthetic promoter; P_{LtetO}, a well-known artificial promoter with extremely low basal leakage and negatively regulated by TetR; MBP, mercury binding protein for bioremediation.
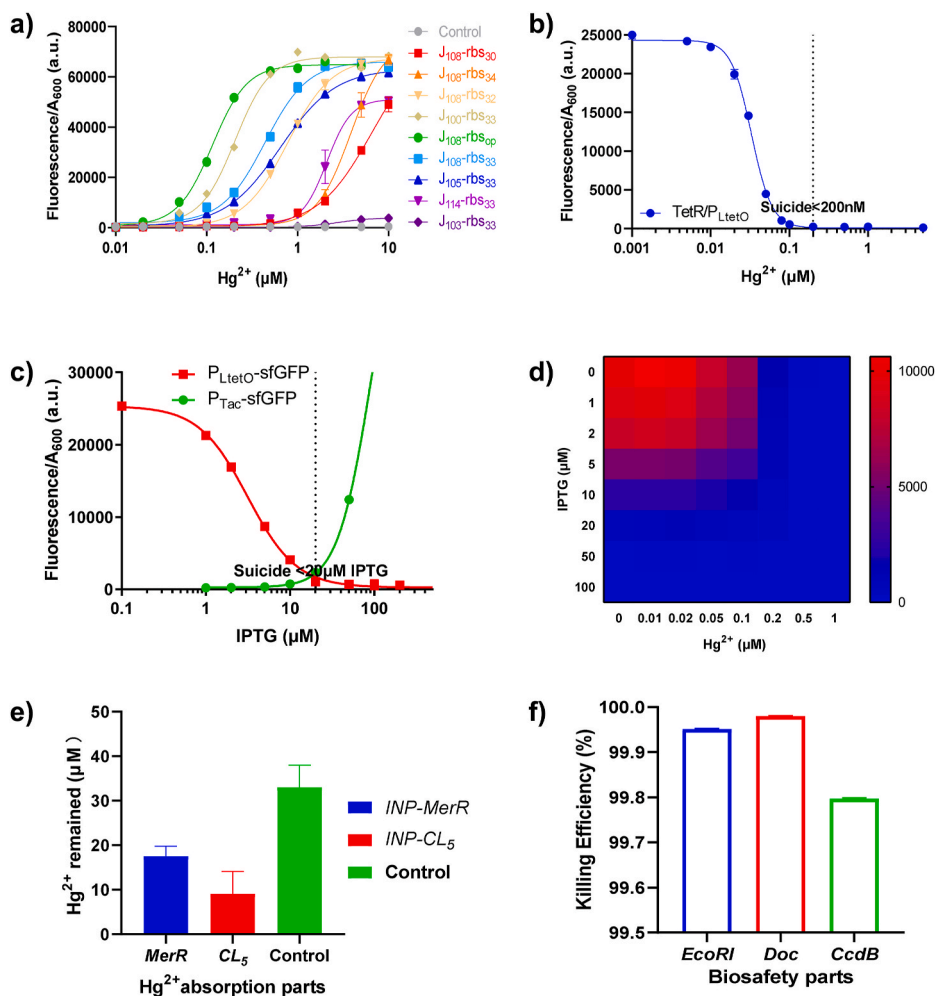
Fig. 2. Response sensitivity optimization of modules in the designed genetic circuit.

a) dose-response curve of Hg^{2+} responsible promoters with different *MerR* strengths; b) architecture of Hg^{2+} repressible NOT logical gates based on TetR transcriptional regulator; c) architecture of IPTG biosensor and IPTG repressible NOT logical gates; d) heatmap of the logic gate with Hg^{2+} and IPTG input; e) selection of appropriate mercury absorption proteins; f) screening of killing genes with high efficiencies. Values are mean ± SD ($n = 3$ biologically independent experiments).

Table 2

Best fits of MerR-P_{MerT} with various promoter and RBS pairs.

Sensors	Inducer	k(a.u.)	α	n	K_m (μM)	R^2
J103-33MerR-P_{MerT}-sfGFP	Hg (NO$_3$)$_2$	3957 ± 82	0.6448 ± 0.1163	2.3520 ± 0.1365	2.8240 ± 0.1025	0.9991
J114-33MerR-P_{MerT}-sfGFP	Hg (NO$_3$)$_2$	51094 ± 2595	0.2443 ± 0.4993	3.2150 ± 1.1040	2.0900 ± 0.1720	0.9888
J105-33MerR-P_{MerT}-sfGFP	Hg (NO$_3$)$_2$	63223 ± 643	0.004483 ± 0.0036	1.4380 ± 0.0560	0.6455 ± 0.0180	0.9996
J108-33MerR-P_{MerT}-sfGFP	Hg (NO$_3$)$_2$	66077 ± 1423	0.006113 ± 0.0043	1.8560 ± 0.2130	0.4388 ± 0.0306	0.9965
J108-RBSop-MerR-P_{MerT}-sfGFP	Hg (NO$_3$)$_2$	64874 ± 832	0.00009113 ± 0.00013336	2.2930 ± 0.2105	0.1159 ± 0.0048	0.9982
J100-33MerR-P_{MerT}-sfGFP	Hg (NO$_3$)$_2$	67970 ± 1411	0.0005805 ± 0.00073995	2.3060 ± 0.3385	0.2056 ± 0.0148	0.9948
J108-32MerR-P_{MerT}-sfGFP	Hg (NO$_3$)$_2$	67486 ± 1231	0.001441 ± 0.007176	1.7890 ± 0.1345	0.7789 ± 0.0348	0.9984
J108-34MerR-P_{MerT}-sfGFP	Hg (NO$_3$)$_2$	74229 ± 5032	0.2213 ± 0.3441	2.3230 ± 0.3350	3.8330 ± 0.3580	0.9948
J108-30MerR-P_{MerT}-sfGFP	Hg (NO$_3$)$_2$	74967 ± 16482	0.06485 ± 0.1527	1.4780 ± 0.2415	6.5000 ± 2.2480	0.9954
J100-33MerR-P_{MerT}-30HrpRS-t-pHrpL-sfGFP	Hg (NO$_3$)$_2$	12813 ± 471	0.0000009544 ± 0.0000047515	0.9354 ± 0.1164	0.00006657 ± 0.00000891	0.9906
J108-rbsop-MerR-P_{MerT}-30HrpRS-t-pHrpL-sfGFP	Hg (NO$_3$)$_2$	11671 ± 480	−5.4600E-7 ± 3.6516E-6	0.9856 ± 0.1412	0.00003495 ± 0.000005695	0.9846
J103-33MerR-P_{MerT}-sfGFP	Hg (NO$_3$)$_2$	3957 ± 82	0.6448 ± 0.1163	2.3520 ± 0.1365	2.8240 ± 0.1025	0.9991
J114-33MerR-P_{MerT}-sfGFP	Hg (NO$_3$)$_2$	51094 ± 2595	0.2443 ± 0.4993	3.2150 ± 1.1040	2.0900 ± 0.1720	0.9888

Values of k, α, n and K_m are mean with 95% confidence intervals. Each curve was fitted by at least 3 biologically independent experiments.

calculated strength of approximately 150 arbitrary units (a.u.) (https://salislab.net/software), which is slightly lower than the commonly used weak RBS B0033 (rbs_{33}) (Wang et al., 2013). We experimentally verified this promoter and RBS pair to be the best combination of mercury sensor with a relative high sensitivity and swift switch between ON and OFF states. Notably, the mercury sensor sensitivity was improved only by tuning the intercellular protein expression without changing the gene sequence. Thus, the specificity of MerR for Hg^{2+} will not alter. Additionally, no fluorescence was observed when no Hg^{2+} was added, which also indicated the functional protein expressed by this genetic circuit is indeed specifically expressed for Hg^{2+}.

Next, we constructed a NOT gate as an inverter circuit to allow activation of cell death without additional inducers in natural environment. Traditional gene regulation based on 'inducible system' or 'quorum sensing' are able to achieve dynamic control of certain biological functions through sophisticated design of genetic circuits that enable complex spatial and temporal regulation of cell death related gene expression. However, once applied to real-life biocontainment systems, cell death could only be trigger with the help of additional small molecules inducers, named 'Active Containment' (Li and Wu, 2009), which is actually impractical under realistic surroundings. Meanwhile, biological NOT gates, which are generally presented as a transcriptional-based NOT gate (Wang and Buck, 2012), formed the basic function of information processing in variety of genetic circuits, which provides an alternative solution. Here, with the multiple-input logic gates, our "intelligent cell" can achieve programmed cell death without any other inducer (Fig. 1). We implemented this idea using the well-known IPTG regulated gene expression system (Sensor 2 part in Fig. 1) in tandem with a commonly used transcriptional repressor TetR, who tightly governs the transcription of a downstream P_{LtetO} promoter. Both of the input P_{Tac} promoter and output P_{LtetO} promoter formed an IPTG rigorously repressible NOT gate. Similarly, *sf*GFP was used as a reporter gene. We tested strain harboring this circuit in LB supplemented with IPTG gradient from 0 to 500 μM. With the presence of at least 20 μM IPTG, *sf*GFP gene expression under control of P_{LtetO} promoter were tightly closed (Fig. 2c), thus providing the feasibility of operating toxic genes in the strains harboring this circuits.

NOR logic gates are "functionally complete", which means any complicated logical computations could be built by combining multiple NOR gates. Plenty of NOR gates with various architectures have been designed and characterized among *E. coli* (Tamsir et al., 2011). Here, we used the well characterized TetR and its cognate promoter to construct a simplified NOR logical gate (Fig. 1). We tested the synthetic circuit with NOR-operation function under four conditions: (1) 500 μM IPTG, (2) 500 nM Hg^{2+}, (3) 500 μM IPTG, and (4) 500 nM Hg^{2+}. To determine the precise dose of inducers needed to switch the NOR gate to ON state, more combinations of IPTG and Hg^{2+} gradients were tested. As is shown in Fig. 2d, the NOR gate synthetic circuit performed as expected. Twenty μM IPTG or 200 nM Hg^{2+} was sufficient to maintain strain alive. Consequently, it means that at least 20 μM IPTG is required to be added in the seed culture stage. Moreover, when the environmental Hg^{2+} concentration dropped beneath the industrial effluent quality standard (250 nM), the biocontainment system could be turned on automatically.

After optimization of the sensitivity and performance of the genetic circuit, the Hg^{2+} treatment elements were also screened. Considering the nondegradable character of heavy metal elements, bio-adsorption and recovery strategies should provide a feasible way to completely remove heavy metals from environment, in order to prevent secondary pollution (Lata et al., 2015). Microorganisms absorb and detoxify heavy metal ions through various mechanisms, one of which is through endogenous proteins that could bind to heavy metal ions. For example, the MerR protein, which can be found in commonly seen bacterial species including *P. aeruginosa*, *B. megaterium* and *S. aureus*, is capable of binding to Hg^{2+} ion with high specificity (Wang et al., 2016). Thus, the efficient mercury absorption were first mined from recently reports (Bae et al., 2003; Liu et al., 2019). Finally, two adsorption proteins, MerR and

polypeptide of $(Cys-Lys)_5$ (CL_5), were selected, as shown in Fig. 2e. Surface-displayed polypeptides CL_5, by using N-terminal of ice-nucleation protein (INP-N) from *P. syringae* as the anchor protein (Li et al., 2004), could efficiently remove the majority of Hg^{2+} with an absorption rate of >80% when the initial cell density was approximately 1×10^9 CFU/mL. Thus, CL_5 was selected for the subsequent experiments.

Finally, the last element in the circuit is the suicide gene. For a better killing efficiency, we firstly screened several toxin genes with different cell killing mechanism. Besides *Eco*RI endonuclease, the DNA gyrase inhibitor CcdB and 30S ribosomal subunit inhibitor Doc were placed under the tightly regulated promoter P_{LtetO}. Escapee rates were calculated via dotting assay under permissive and non-permissive conditions. The toxin with the highest biocontainment ability turned out to be the *doc* gene who inhibit strain's protein translation and thus caused a rapidly arrest of the living strains (Fig. 2f). Intercellular accumulation of Doc protein provides efficient cell killing capability with a ratio of cell death measured no less than 99.99%. The reason is probably that the combined impacts of destruction of DNA integrality as well as deactivation of protein synthesis are better than inhibition of DNA replication, the basis of *ccdB*. Additionally, *Eco*RI endonuclease also performed well by cutting the *E. coli* chromosome into pieces and thus makes cells almost impossible to stay alive.

3.3. Mercury recovery by magnetically immobilized cells with biosecurity circuit

Using the optimized modules, we engineered a *E. coli* strain with programmable capability of Hg^{2+} adsorption and cell death. However, efficient removal of waterbody heavy metal pollution also requires non-biology methods to enhance the stability of biocatalyst as well as the reusable feasibility of absorbing cells. For this purpose, immobilization of cells has shown its advantages comparing to free cells. Specifically, microbial immobilization on magnetic nanoparticles provided a simplified way for rapid recovery, which is also a cost-effective way of adsorption and desorption circulation process for recovery of environmental contaminants (Yang et al., 2014). Additionally, magnetic nanoparticles are superparamagnetic with a large surface area, which reduces the mass transfer resistance in traditional immobilization processes. Such magnetic materials are easily accessible because they have been widely used in various fields, including environmental remediation and biotransformation processes (Liu and Yu, 2015). Here, we attempted to use appropriate magnetic nanoparticles to construct calcium alginate immobilized cells.

Moreover, we selected the appropriate magnetic material for immobilization process. Fe(0) and Fe (II) are able to reduce Hg(II) to Hg (0) since the oxidation-reduction potential of Fe(0) and Fe (II) are lower than Hg(II), and the resulting Hg(0) could escape into the atmosphere (Rodríguez-Raposo et al., 2000). Pre-experiments also showed that the excessive Fe(II), which is abundant in Fe_3O_4 nanoparticles, has reduction activity towards Hg^{2+} and thus made Fe_3O_4 unsuitable as the magnetic material (Fig. 3a). Therefore, we selected strontium ferrite ($SrFe_{12}O_{19}$) to substitute Fe_3O_4 because of its chemical inertness of Fe (III) towards Hg (II) (Volodchenkov et al., 2016). Then, we devised a strategy for reducing mercury pollution with reusable magnetic material, which can easily recycle Hg^{2+} through one-step elution. Specifically, magnetic surface display of artificial *E. coli* harboring entire genetic circuit with $INP-CL_5$ gene were performed (Fig. 3b). The initial cell density in the magnetically immobilized particles was also optimized. When the initial cell density was improved to 10^{10} CFU, the immobilized cells showed an efficient mercury binding capacity up to 98% under an initial Hg^{2+} concentration of 50 μM. The mercury adsorption equilibrium time was previously reported to be within 1 h for free *E. coli* cells harboring Hg^{2+} adsorption protein (Liu et al., 2019). In our experiments, it took about 2 h for reaching an adsorption equilibrium (Fig. 3b). This might be due to the immobilized materials, alginate,
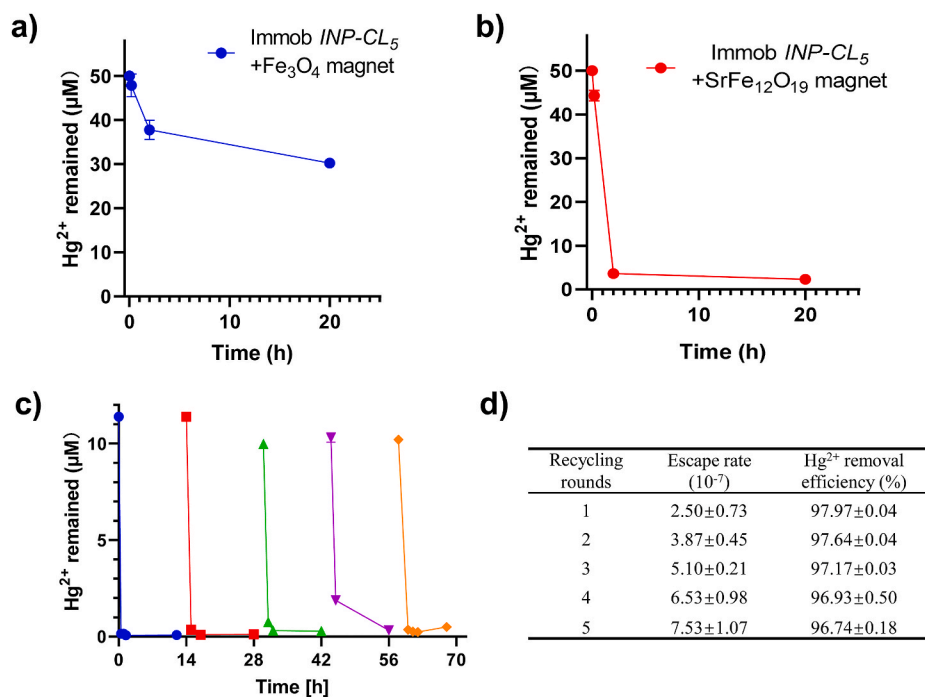
Fig. 3. Mercury recovery by repeatedly using magnetically immobilized cells with bioremediation and biocontainment system.
The pre-experiments of mercury absorption efficiency by immobilized cells using Fe_3O_4 (a) or $SrFe_{12}O_{19}$ (b) as magnetically nanoparticles; c) the adsorption efficiencies of repeated used magnetically immobilized cells; d) the accurate data of anti-escape and Hg^{2+} removal rates in each cycle.

which inhibited the diffusion of Hg^{2+} as compared to that of free cells.

Additionally, in an industrial bioremediation process, recycle of biocatalysts could be an important factor that determines the effectiveness of degradation over time. With magnetic properties, the biocatalysts will be easily collected from aqueous phase by an external magnetic field, thus making the recovery process more feasible and cost-effective. In the multiple cycles of mercury absorption test, mercury binding peptide CL5 showed a maximum capacity of 3.8 mg/g dry weight, and mercury removal efficiency could maintain at no less than 95% for at least 5 rounds of repeated usage (Fig. 3c). The escape rates of engineered strains with 2 copies of suicide modules were measured and an approximate 5×10^{-7} escape rate was achieved in each cycle
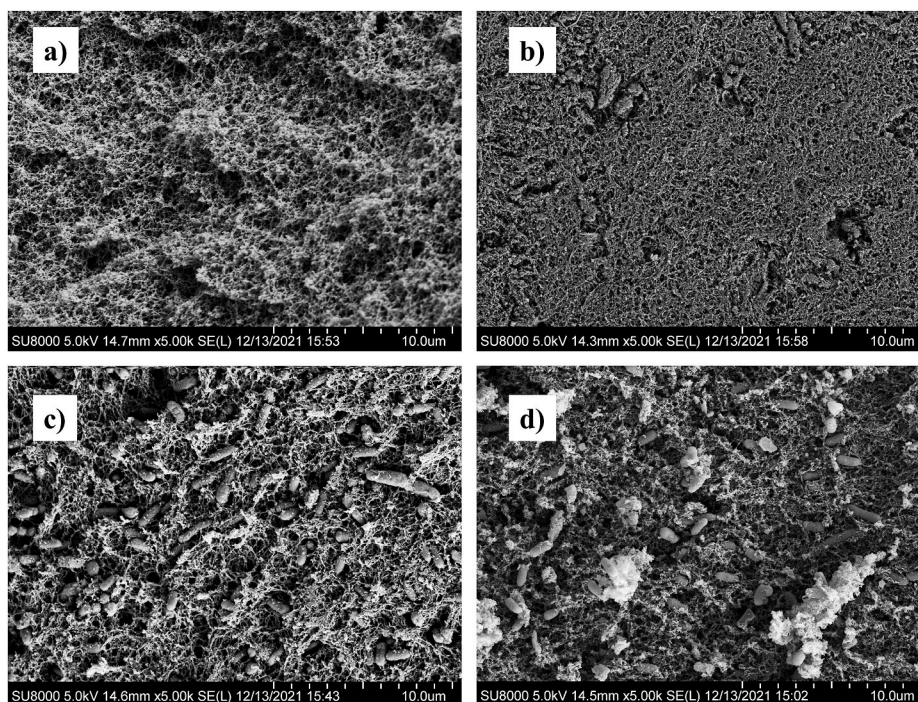

Fig. 4. Scanning electron microscopy (SEM) characterization of the surface properties of strain *E. coli* SS V3.0 cells loaded with magnetic nanomaterials.
a) internal structure of magnetic material without cells; b) external structure of magnetic material without cells; c) internal surface properties of magnetically immobilized cells; and d) external surface of cells loaded with magnetic nanomaterials.

(Fig. 3d). The surface property of cells loaded with magnetic nanomaterials was characterized by scanning electron microscope. The interior and exterior surface properties of magnetic nanomaterials with alginate except the bacteria were denoted as the negative control (Fig. 4a & **4b**). The sample results depicted that on the both internal and external surface of magnetically immobilized beads, visible strains and magnetic nanomaterials were well attached onto the microstructure of alginate-based materials (Fig. 4c & **4d**). The irregular crystals in the high-brightness and high-electron density regions are $SrFe_{12}O_{19}$ nano-magnetic particles. The strains were enveloped in the pores formed by calcium alginate and the number of cells embedded in the inner surface was obviously more than that on the outer surface. The inner surface of the calcium alginate magnetic beads embedded with strains had a larger porosity than the outer surface and could accommodate more bacterial cells for Hg^{2+} adsorption. This property could well explain the high efficiency of Hg^{2+} adsorption by the magnetic immobilized cells.

3.4. Improving the anti-escape rate by optimizing the killing module

NIH guideline recommended that GMO escape rate should be guaranteed under 10^{-8}, thus requiring further reduction of escape rate of the engineered strain. One way to achieve such goal is to introduce the auxotroph strategy. For example, the chassis *E. coli* TOP10 is leucine auxotroph and DH5α is thiamine and arginine auxotroph (Durfee et al., 2008). However, the high costs associated with supplementing the essential amino acids or other metabolites in natural environment dramatically limits the application of such strains (Arnolds et al., 2021). Alternatively, redundant strategy could be an appreciative substitute biocontainment system with ultra-security. Thus, we constructed a redundant system with 2 copies of *doc* and one copy of *ecoRI* gene in the engineered mercury recovery strain to achieve high biocontainment efficiency.

To avoid excessive metabolic burden, the compatible low copy number plasmids pSEVA221 and pSBAC were used as the backbone. The toxin gene *doc* driven by promoter P_{LtetO} was subcloned onto these two plasmids for additional copies of biocontainment systems (Fig. 5a), resulting in the recombinant plasmids pSEVA221-*pLtetO-doc* and pBAC-*LtetO-doc* for constructing the biosecurity strain. As shown in Fig. 5b, strain with one additional copy of killing gene could only maintain survive one of 10 million. The lowest escape rate of $<10^{-9}$ was achieved with three copies of toxin gene, which meets the NIH guideline for GMOs environmental release. The final strain with whole gene circuit, named *E. coli* SS V3.0, was applied to Hg^{2+} adsorption again with the magnetic immobilization process by fixing 10 mL (10 OD/mL) cells on the calcium alginate beads (approximately 100 billion CFUs used per test). According to the NIH standard, no more than 1000 CFUs should be detected on removal of Hg^{2+}. The escapers were detected after all the water phase was collected by centrifugation after 12 h of absorption. The resulting pellets were plated onto LB agar culture dishes for detecting the escape rates. The stability of this strain was confirmed in long periods of immobilized experiments. The results showed that the magnetically immobilized cells displayed a removal efficiency of no less than 95% for 5 cycles but dropped to 70% in the sixth round, which indicated the cells become to decline (data not shown). The escape rates were kept below 10^{-9} for 5 cycles with an average escape rate of $(0.81 \pm 0.06) \times 10^{-9}$ (Fig. 5c), which is below the recommendation demand of U.S. NIH guideline ($<10^{-8}$). Given the feasibility of separation by an external magnetic field and high adsorption efficiency, this study provides a promising technique for mercury remediation in wastewater using GMOs.

4. Conclusions

Environmental pollution has become a serious global problem. The engineered strains with high efficiency will definitely make great contributions for a clean world. However, bio-threats from GMOs released into environments has hindered its application. To date, researchers rarely demonstrated the theories of genetic safeguard systems. In this
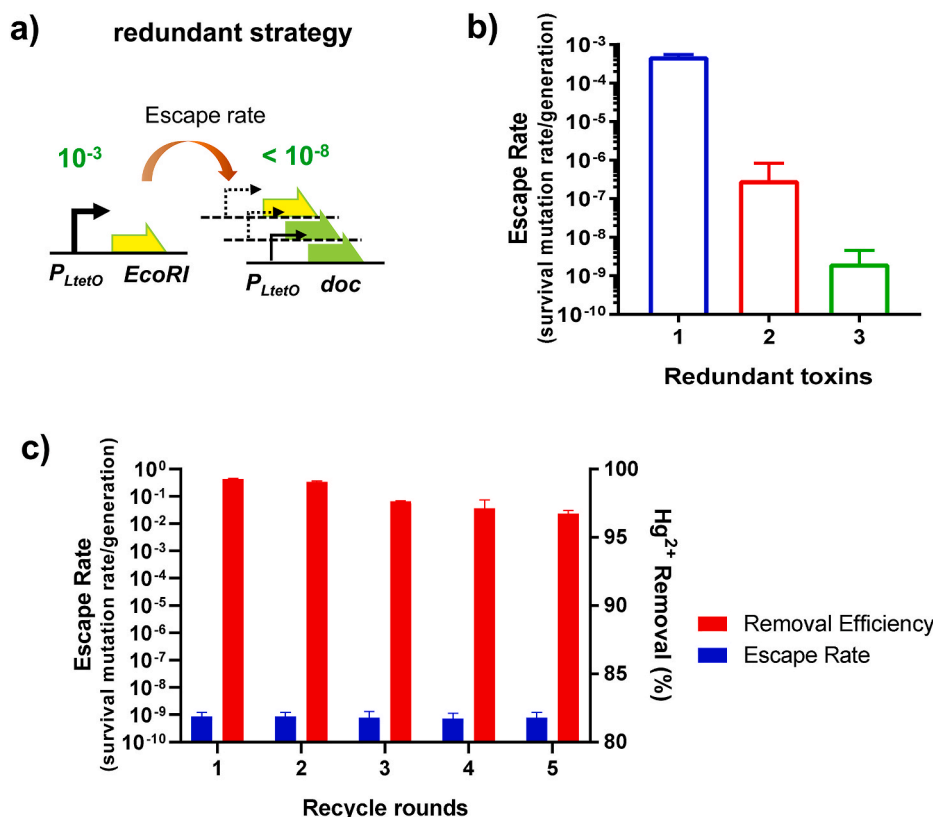

Fig. 5. Further improving the anti-escape performance by toxin redundant strategy in the final engineered strain *E. coli* SS V3.0.

a) Schematic of redundant strategy for improving the killing efficiency; b) the killing efficiencies of strains with different copies of toxin genes; c) the escape rates and Hg^{2+} removal efficiencies of magnetically immobilized cells in 5 round testing. The escape rate was defined as the overall survival rate of strains during cultivation without IPTG or Hg^{2+} and the control was the cell counting number on the plate with IPTG to suppress the toxin gene expression.

study, we developed a synthetic biology approach to control the behavior of GMOs. The strain with optimized genetic circuit could sense the variation of Hg^{2+} concentration in waterbody and automatically trigger programmable cell death after completion of the mission. The designed circuit endowed strains with an escape rate of less than 10^{-9}, which is below the U.S. NIH guideline demand for GMO release into the environments. Thus, this study provides a promising technology in bioremediation fields to directly apply engineered microbes in an open environment.

CRediT authorship contribution statement

Yubin Xue: Data curation, Writing – original draft, preparation. **Pei Du:** Software, Validation. **Amal Amin Ibrahim Shendi:** Writing – review & editing. **Bo Yu:** Conceptualization, Supervision.

Declaration of competing interest

The authors declare that they have no known competing financial interests or personal relationships that could have appeared to influence the work reported in this paper.

Acknowledgments

References

Arnolds, K.L., Dahlin, L.R., Ding, L., et al., 2021. Biotechnology for secure biocontainment designs in an emerging bioeconomy. Curr. Opin. Biotechnol. 71, 25–31. https://doi.org/10.1016/j.copbio.2021.05.004.

Bae, W., Wu, C.H., Kostal, J., et al., 2003. Enhanced mercury biosorption by bacterial cells with surface-displayed MerR. Appl. Environ. Microbiol. 69 (6), 3176–3180. https://doi.org/10.1128/AEM.69.6.3176-3180.2003.

Brown, N.L., Stoyanov, J.V., Kidd, S.P., et al., 2003. The *MerR* family of transcriptional regulators. FEMS Microbiol. Rev. 27 (2–3), 145–163. https://doi.org/10.1016/S0168-6445(03)00051-2.

Brune, K.D., Bayer, T.S., 2012. Engineering microbial consortia to enhance biomining and bioremediation. Front. Microbiol. 3, 203. https://doi.org/10.3389/fmicb.2012.00203.

Cerminati, S., Soncini, F.C., Checa, S.K., 2015. A sensitive whole-cell biosensor for the simultaneous detection of a broad-spectrum of toxic heavy metal ions. Chem. Commun. 51, 5917–5920. https://doi.org/10.1039/C5CC00981B.

Cui, Y.L., Chen, Y.C., Liu, X.Y., et al., 2021. Computational redesign of a PETase for plastic biodegradation under ambient condition by the GRAPE Strategy. ACS Catal. 11, 1340–1350. https://doi.org/10.1021/acscatal.0c05126.

Dana, G.V., Kuiken, T., Rejeski, D., 2012. Synthetic biology: Four steps to avoid a synthetic-biology disaster. Nature 483, 29. https://doi.org/10.1038/483029a.

Durfee, T., Nelson, R., Baldwin, S., et al., 2008. The complete genome sequence of *Escrichia coli* DH10B: insights into the biology of a laboratory workhorse. J. Bacteriol. 190 (7), 2597–2606. https://doi.org/10.1128/JB.01695-07.

Engler, C., Kandzia, R., Marillonnet, S., 2008. A one pot, one step, precision cloning method with high throughput capability. PLoS One 3 (11), e3647. https://doi.org/10.1371/journal.pone.0003647.

Gibson, D.G., Young, L., Chuang, R.Y., et al., 2009. Enzymatic assembly of DNA molecules up to several hundred kilobases. Nat. Methods 6 (5), 343–345. https://doi.org/10.1038/nmeth.1318.

Hossain, A., Lopez, E., Halper, S.M., et al., 2020. Automated design of thousands of nonrepetitive parts for engineering stable genetic systems. Nat. Biotechnol. 38 (12), 1466–1475. https://doi.org/10.1038/s41587-020-0584-2.

Khalil, A.S., Collins, J.J., 2010. Synthetic biology: applications come of age. Nat. Rev. Genet. 11 (5), 367–379. https://doi.org/10.1038/nrg2775.

Lata, S., Singh, P.K., Samadder, S.R., 2015. Regeneration of adsorbents and recovery of heavy metals: a review. Int. J. Environ. Sci. Technol. 12, 1461–1478. https://doi.org/10.1007/s13762-014-0714-9.

Li, L., Gyun Kang, D., Joon Cha, H., 2004. Functional display of foreign protein on surface of *Escherichia coli* using N-terminal domain of ice nucleation protein. Biotechnol. Bioeng. 85, 214–221. https://doi.org/10.1002/bit.10892.

Li, Q., Wu, Y.J., 2009. A fluorescent, genetically engineered microorganism that degrades organophosphates and commits suicide when required. Appl. Microbiol. Biotechnol. 82 (4), 749–756. https://doi.org/10.1007/s00253-009-1857-3.

Liu, F., Yu, B., 2015. Efficient production of reuterin from glycerol by magnetically immobilized *Lactobacillus reuteri*. Appl. Microbiol. Biotechnol. 99 (11), 4659–4666. https://doi.org/10.1007/s00253-015-6530-4.

Liu, M., Zhang, Y., Inouye, M., et al., 2008. Bacterial addiction module toxin *Doc* inhibits translation elongation through its association with the 30S ribosomal subunit. Proc. Natl. Acad. Sci. U. S. A 105 (15), 5885–5890. https://doi.org/10.1073/pnas.0711949105.

Liu, M., Kakade, A., Liu, P., et al., 2019. Hg^{2+}-binding peptide decreases mercury ion accumulation in fish through a cell surface display system. Sci. Total Environ. 659, 540–547. https://doi.org/10.1016/j.scitotenv.2018.12.406.

Lutz, R., Bujard, H., 1997. Independent and tight regulation of transcriptional units in *Escherichia coli* via the LacR/O, the TetR/O and AraC/I1-I2 regulatory elements. Nucleic Acids Res. 25 (6), 1203–1210. https://doi.org/10.1093/nar/25.6.1203.

Moe-Behrens, G.H., Davis, R., Haynes, K.A., 2013. Preparing synthetic biology for the world. Front. Microbiol. 4, 5. https://doi.org/10.3389/fmicb.2013.00005.

Özyurt, C., Üstükarcı, H., Evran, S., et al., 2019. MerR-fluorescent protein chimera biosensor for fast and sensitive detection of Hg^{2+} in drinking water. Biotechnol. Appl. Biochem. 66 (5), 731–737. https://doi.org/10.1002/bab.1805.

Pant, G., Garlapati, D., Agrawal, U., et al., 2021. Biological approaches practised using genetically engineered microbes for a sustainable environment: a review. J. Hazard. Mater. 5 (405), 124631. https://doi.org/10.1016/j.jhazmat.2020.124631.

Quist, D., Chapela, I.H., 2001. Transgenic DNA introgressed into traditional maize landraces in Oaxaca, Mexico. Nature 414 (6863), 541–543. https://doi.org/10.1038/35107068.

Rodríguez-Raposo, R., Meléndez-Hevia, E., Spiro, M., 2000. Autocatalytic formation of colloidal mercury in the redox reaction between Hg^{2+} and Fe^{2+} and between Hg_2^{2+} and Fe^{2+}. J. Mol. Catal. Chem. 164 (1–2), 49–59. https://doi.org/10.1016/S1381-1169(00)00203-X.

Redford, K.H., Adams, W., Mace, G.M., 2013. Synthetic biology and conservation of nature: wicked problems and wicked solutions. PLoS Biol. 11 (4), e1001530 https://doi.org/10.1371/journal.pbio.1001530.

Redford, K.H., Brooks, T.M., Macfarlane, N., et al., 2019. Genetic Frontiers for Conservation: an Assessment of Synthetic Biology and Biodiversity Conservation. IUCN, Switzerland. https://doi.org/10.2305/IUCN.CH.2019.05.en.

Sayler, G.S., Ripp, S., 2000. Field applications of genetically engineered microorganisms for bioremediation processes. Curr. Opin. Biotechnol. 11 (3), 286–289. https://doi.org/10.1016/s0958-1669(00)00097-5.

Smith, A.B., Maxwell, A., 2006. A strand-passage conformation of DNA gyrase is required to allow the bacterial toxin, *CcdB*, to access its binding site. Nucleic Acids Res. 34 (17), 4667–4676. https://doi.org/10.1093/nar/gkl636.

St-Pierre, F., Cui, L., Priest, D.G., et al., 2013. One-step cloning and chromosomal integration of DNA. ACS Synth. Biol. 2 (9), 537–541. https://doi.org/10.1021/sb400021j.

Tamsir, A., Tabor, J., Voigt, C., 2011. Robust multicellular computing using genetically encoded NOR gates and chemical 'wires'. Nature 469, 212–215. https://doi.org/10.1038/nature09565.

Tao, H.C., Peng, Z.W., Li, P.S., et al., 2013. Optimizing cadmium and mercury specificity of *CadR*-based *E. coli* biosensors by redesign of *CadR*. Biotechnol. Lett. 35 (8), 1253–1258. https://doi.org/10.1007/s10529-013-1216-4.

Tay, P., Nguyen, P.Q., Joshi, N., 2017. A synthetic circuit for mercury bioremediation using self-assembling functional amyloids. ACS Synth. Biol. 6, 1841–1850. https://doi.org/10.1021/acssynbio.7b00137.

Terpe, K., 2006. Overview of bacterial expression systems for heterologous protein production: from molecular and biochemical fundamentals to commercial systems. Appl. Microbiol. Biotechnol. 72 (2), 211–222. https://doi.org/10.1007/s00253-006-0465-8.

Torres, B., Jaenecke, S., Timmis, K.N., et al., 2003. A dual lethal system to enhance containment of recombinant micro-organisms. Microbiology 149, 3595–3601. https://doi.org/10.1099/mic.0.26618-0.

Volodchenkov, A., Kodera, Y., Garay, J.E., 2016. Synthesis of strontium ferrite/iron oxide exchange coupled nano-powders with improved energy product for rare earth free permanent magnet applications. J. Mater. Chem. C. 4, 5593–5601. https://doi.org/10.1039/C6TC01300G.

Wan, X., Volpetti, F., Petrova, E., et al., 2019. Cascaded amplifying circuits enable ultrasensitive cellular sensors for toxic metals. Nat. Chem. Biol. 15, 540–548. https://doi.org/10.1038/s41589-019-0244-3.

Wang, B., Buck, M., 2012. Customizing cell signaling using engineered genetic logic circuits. Trends Microbiol. 20 (8), 376–384. https://doi.org/10.1016/j.tim.2012.05.001.

Wang, B., Barahona, M., Buck, M., 2013. A modular cell-based biosensor using engineered genetic logic circuits to detect and integrate multiple environmental signals. Biosens. Bioelectron. 40 (1), 368–376. https://doi.org/10.1016/j.bios.2012.08.011.

Wang, D., Huang, S., Liu, P., et al., 2016. Structural analysis of the Hg(II)-Regulatory protein Tn501 MerR from Pseudomonas aeruginosa. Sci. Rep. 6, 33391. https://doi.org/10.1038/srep33391.

Wilson, D.J., 1993. NIH guidelines for research involving recombinant DNA molecules. Account. Res. 3 (2–3), 177–185. https://doi.org/10.1080/08989629308573848.

Wu, G., Yan, Q., Jones, J.A., et al., 2016. Metabolic burden: cornerstones in synthetic biology and metabolic engineering applications. Trends Biotechnol. 34 (8), 652–664. https://doi.org/10.1016/j.tibtech.2016.02.010.

Yang, J., Zou, P., Yang, L., 2014. A comprehensive study on the synthesis and paramagnetic properties of PEG-coated Fe_3O_4 nanoparticles. Appl. Surf. Sci. 303, 425–432. https://doi.org/10.1016/j.apsusc.2014.03.018.

Zhang, W., Zhang, X., Tian, Y., et al., 2018. Risk assessment of total mercury and methylmercury in aquatic products from offshore farms in China. J. Hazard Mater. 354, 198–205. https://doi.org/10.1016/j.jhazmat.2018.04.039.

Zhu, N., Zhang, B., Yu, Q., 2020. Genetic engineering-facilitated coassembly of synthetic bacterial cells and magnetic nanoparticles for efficient heavy metal removal. ACS Appl. Mater. Interfaces 12 (20), 22948–22957. https://doi.org/10.1021/acsami.0c04512.

Zong, Y., Zhang, H.M., Lyu, C., et al., 2017. Insulated transcriptional elements enable precise design of genetic circuits. Nat. Commun. 8 (1), 52. https://doi.org/10.1038/s41467-017-00063-z.